PNNL-31959 Rev 0
DVZ-RPT-065 Rev 0

Combined Technologies for In Situ Remediation of Tc-99 and U in Subsurface Sediments

September 2021

BN Gartman
ES Arnold
JE Szecsody
C Bagwell
CF Brown
SA Saslow
CI Pearce
VL Freedman
NP Qafoku

Prepared for the U.S. Department of Energy
under Contract DE-AC05-76RL01830

PACIFIC NORTHWEST NATIONAL LABORATORY
operated by
BATTELLE
for the
UNITED STATES DEPARTMENT OF ENERGY
under Contract DE-AC05-76RL01830

Printed in the United States of America

Available to DOE and DOE contractors from the
Office of Scientific and Technical Information,
P.O. Box 62, Oak Ridge, TN 37831-0062;
ph: (865) 576-8401
fax: (865) 576-5728
email: reports@adonis.osti.gov

Available to the public from the National Technical Information Service
5301 Shawnee Rd., Alexandria, VA 22312
ph: (800) 553-NTIS (6847)
email: orders@ntis.gov <https://www.ntis.gov/about>
Online ordering: http://www.ntis.gov

PNNL-31959 Rev 0
DVZ-RPT-065 Rev 0

Combined Technologies for In Situ Remediation of Tc-99 and U in Subsurface Sediments

September 2021

BN Gartman
ES Arnold
JE Szecsody
C Bagwell
CF Brown
SA Saslow
CI Pearce
VL Freedman
NP Qafoku

Prepared for
the U.S. Department of Energy
under Contract DE-AC05-76RL01830

Pacific Northwest National Laboratory
Richland, Washington 99354

Summary

In this study, combinations of chemical remedies were tested in bench-scale batch experiments to evaluate a two-step reduction-sequestration approach to effectively stabilize high concentrations of inorganic contaminant mixtures. Bench tests simulated contaminant and geochemical conditions of a perched aquifer located within the Central Plateau at the Hanford Site, located in southeastern Washington State (USA). Pairwise combinations of a reductant [e.g., zero valent iron, sulfur modified iron (SMI), or calcium polysulfide] and a sequestering agent [e.g., calcite, apatite, or dilute alkaline solution (e.g., NaOH)] were evaluated for immobilization and stabilization of technetium (Tc) (50,000 pCi/L), uranium (U) (150 mg/L), and nitrate (NO_3) (200 mg/L) in high ionic strength groundwater.

The results of these batch studies demonstrated that reduction by SMI and sequestration in apatite or calcite are the most effective combination for these contaminant mixtures and conditions. Aqueous concentrations of Tc and U decreased by 95.6% ± 2.5% and 101.1% ± 5.2%, respectively, with SMI-apatite and 98.3% ± 0.0% and 101.2% ± 5.2%, respectively, with SMI-calcite. Sequential extractions showed that sequestered contaminants had limited capacity for re-oxidation; in fact, less than 10% of immobilized Tc and U was recovered by selective extraction of mineral phases most susceptible to oxidation. In addition, X-ray absorption near edge structure analysis of the sediment samples treated with SMI-calcite showed the presence of only U(IV), while both U(IV) and U(VI) were present in the SMI-apatite combination [ratio of 0.43 U(IV):0.59 U(VI)].

This study describes preliminary results that a two-step approach for stabilizing contaminant mixtures of long-lived radionuclides can be effective at reducing contaminant fluxes to groundwater from vadose and perched water zones.

Acknowledgments

The authors would like to thank Steve Heald and Michael Pape for their support at the Advanced Photon Source (APS). This research used resources of the APS, an Office of Science User Facility operated for the U.S. Department of Energy (DOE) by Argonne National Laboratory and was supported by DOE under Contract No. DE-AC02-06CH11357, and the Canadian Light Source and its funding partners.

Funding for this work was provided by the DOE Richland Operations Office under the Deep Vadose Zone – Applied Field Research Initiative. The Pacific Northwest National Laboratory is operated by Battelle Memorial Institute for the Department of Energy under Contract DE-AC05-76RL01830.

Acronyms and Abbreviations

APS	Advanced Photon Source
ASME	American Society of Mechanical Engineers
CCU	Cold Creek Unit
CFR	Code of Federal Regulations
CPS	calcium polysulfide
NQAP	Nuclear Quality Assurance Program
PNNL	Pacific Northwest National Laboratory
SMI	sulfur-modified iron
SPW	synthetic perched water
XAFS	X-ray absorption fine structure
XANES	X-ray absorption near edge structure
ZVI	zero-valent iron

Contents

Figures

Tables

1.0 Introduction

Contamination in the unsaturated vadose zone at many industrial and former nuclear production sites presents a long-term threat to groundwater and potential risk to sensitive receptors (Campbell et al. 2012; Pearce et al. 2018; Truex et al. 2017; Wellman et al. 2008). Remedial strategies for the vadose zone typically include targeted elimination of the contaminant source term, and a reliance on attenuation mechanisms to limit contaminant flux to groundwater (Bagwell et al. 2018; Saslow et al. 2018; Szecsody et al. 2010). However, recalcitrant contaminants with long residence times may require stabilization in place to reduce their flux to groundwater. Because preferential flow path, subsurface heterogeneities, bypassed fractures, and areas of low to no permeability often accumulate contaminants, direct solutions for contaminant mass residing in low-permeability regions are needed. These zones are also responsible for rebound in contaminant concentrations after site cleanup is presumed complete (e.g., Thomson et al. 2008).

A perched aquifer sits beneath the B-Complex in the 200 East Area at the Hanford Site, in southeastern Washington state (Oostrom et al. 2013). Contamination of the vadose zone and the perched aquifer is the result of planned releases from infiltration galleries as well as unplanned releases from the overlying tank farms and associated facilities. The perched zone serves as a continuing source for uranium (U), technetium (Tc), and nitrate (NO_3^-) to the underlying aquifer. Water extraction is the current response action, but the large footprint and low hydraulic conductivity limit the effective removal of contaminants. Therefore, in situ remedial technologies may be needed in combination with flux control measures to properly address the contamination and complexity of this site.

Aqueous transport of redox active radionuclides (e.g., U, Tc) is strongly influenced by redox and pH conditions (Icenhower et al. 2008; Ilton et al. 2008; Liu et al. 2015; Qafoku et al. 2010). As such, subsurface biogeochemical conditions can be intentionally manipulated to promote reductive precipitation or adsorption to decrease the solubility of these radionuclides (Szecsody et al. 2004). However, reduced oxidation states for most radionuclides are prone to rapid re-oxidation as natural oxidative conditions reestablish. For example, groundwater concentrations of uranium were successfully depleted by in-situ biostimulation at the Oak Ridge Field Research Center (TN, USA) and at the Old Rifle Site (CO, USA); however, rapid re-oxidation resulted in remobilization once nutrient additions, and bioreduction, ceased (N'Guessan et al. 2010; Wu et al. 2007). Previous studies have also shown that pertechnetate can be readily bioreduced to $Tc(IV)O_2 \times xH_2O$ (Istok et al. 2004; Fredrickson et al. 2009), a precipitate that can be quickly and nearly completely reoxidized. Tc precipitated with sulfide oxidizes more slowly (i.e., months; Lukens et al. 2002, 2005; Ferrier et al. 2013), but still oxidize.

Because these effects are temporary, reductive immobilization of certain metals and radionuclides is only part of a long-term remedial strategy for contaminated sites. Stabilization measures are required to meaningfully retard or prevent eventual re-oxidation and re-mobilization of radionuclides such as U and Tc. Temporarily reduced Tc(IV) precipitate has been shown by X-ray absorption near edge structure (XANES) surface phase analysis to be stable under oxic conditions due to coating by aluminosilicates in water-saturated sediments (Szecsody et al. 2014), and is also hypothesized to occur at low water saturation for pertechnetate-laden sediment treated with H_2S and NH_3 gasses (Szecsody et al. 2015). Ammonia gas treatment of unsaturated sediments also results in U(VI) reduction and precipitation and aluminosilicate coatings (Di Pietro et al. 2020; Szecsody et al. 2011).

In this study, systematic bench-scale experiments were conducted to compare the effectiveness of combinations of chemical-based remedial treatments for the stable sequestration of radionuclide contaminant mixtures. The approach first applies a chemical reductant to geochemically transform oxidized (soluble) redox-sensitive radionuclides (i.e., Tc and U) to reduced (insoluble) species, followed by a sequestration treatment that coats or incorporates the radionuclides into precipitate phases to prevent oxidative re-mobilization. The results demonstrate effective stabilization of co-mingled contaminants, which could provide a technical foundation from which a strategy for in situ remediation and stabilization of long-lived contaminants can be based.

2.0 Methods and Materials

2.1 Site Description

The experiments are based on characteristics of the perched water zone at the B-Complex area located at the Hanford Site. The low permeability perching unit is approximately 68.6 m (225 ft) below ground surface and 5 meters above the unconfined aquifer. The volume of the perched aquifer has been estimated from a measured constant height of 3.36 meters over an aerial footprint of 19,175 m^2 and an assumed porosity of 0.252 for a total volume of 1.62 x 10^7 L (Truex et al. 2013). The Cold Creek Unit (CCU) silt (CCUz) in the area with perched water is composed of a lower perching silt (CCUz lower), a high sand content zone (CCUz sand), and upper silt zone (CCUz upper). The underlying Cold Creek Unit gravel (CCUg) contains the regional groundwater aquifer and is underlain by basalt. The B-Complex perched water aquifer contains relatively high concentrations of comingled contaminants; priority species include technetium-99 (^{99}Tc; 50,000 pCi/L), uranium (U; 150 mg/L), and nitrate (NO_3; 1730 mg/L) serving as a source term for contamination to the underlying aquifer.

2.2 Experimental Design

Chemical reductants selected for this study included zero-valent iron (ZVI), sulfur-modified iron (SMI), and calcium polysulfide (CPS) (CaS_x, where x ranges from 3 to 7). The reductive capacity for each reductant was quantified following the method outlined by Augus and Glasser (1985) and Kaplan et al. (2005). The sequestering treatments consisted of forming solutions for apatite or calcite mineral precipitation, or NaOH to catalyze pH dependent through mineral dissolution and re-precipitation of aluminosilicates in the Hanford sediments. A schematic of the experimental design is shown in Figure 2.1.

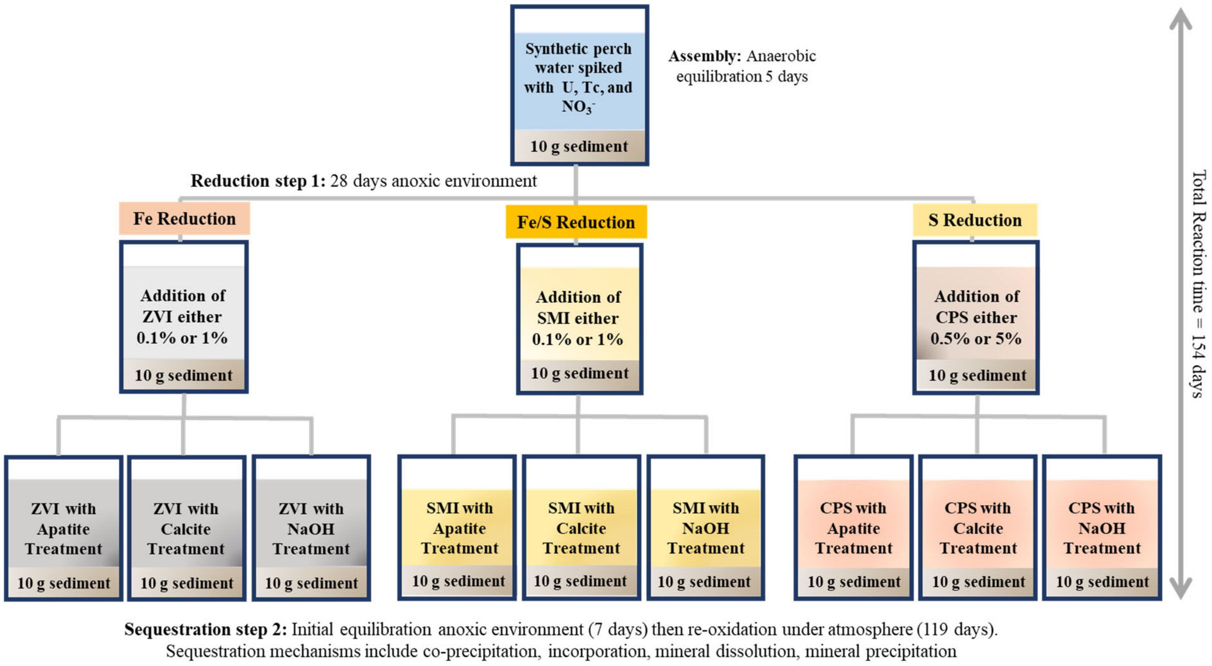

Figure 2.1. Batch reactor reaction scheme for the two-step approach. The depiction of the overall reaction scheme does not include the solution controls, sediment controls, reduction only controls, and sequestration only controls.

2.3 Batch Reactor Setup and Solution Phase Characterization

Contaminated sediment was obtained from borehole C9488 at a depth of 217.3 to 218.3 feet below ground surface from within the CCU at the Hanford Site. The sediment was previously characterized as a sandy mud, with a uranium concentration of 599 µg/kg (Szecsody et al. 2017). Sediments were sieved and the < 2-mm fraction was used. Ten grams of sediment was transferred into 125-mL polycarbonate bottles along with a synthetic perched water (SPW) medium (SPW, 100 mL) for a 1:10 ratio (Table 2.1). Contaminants were spiked into the SPW at site relevant concentrations (i.e., 150 mg/L U, 167 nCi/L TcO_4^-, and 124 mg/L nitrate) and the solution was sparged with N_2 to eliminate oxygen prior to addition in the reactors (DOE/RL-2016-69). Reactor bottles were initially equilibrated for 5 days in an anaerobic chamber with an atmosphere composed of ultrapure argon. Once equilibrated, chemical reductants were added at two concentrations. The ZVI (Hepure FeroxTarget) and SMI (North American Hogan) were both tested at 0.1% and 1.0% by weight, where CPS (29% CPS, Agua-Clear) was added at 0.5% and 5.0% by volume. During the reduction phase of the experiment, aqueous samples were collected at 1 hour and at 7, 13, and 28 days for analysis. Additional samples were collected for the reduction only controls for the duration of the experiment (t=154 days). Samples were filtered with a 0.22-µm polyvinylidene fluoride (PVDF) filter to remove particulates and acidified with concentrated nitric acid (targeting a final nitric concentration of 2%) for analysis of U and Tc by inductively coupled plasma mass spectrometry. Aqueous samples were also analyzed for total cations using a PerkinElmer Optima 3300DV inductively coupled plasma optical emission spectrometry, and anions on a Dionex ICS-2000 ion chromatograph. An Orion pH meter with a Ross combination probe was used to monitor pH changes for all batch systems.

Table 2.1. Synthetic perched water recipe, for 1 L of solution where the final pH is ~8.2 (adjust with 2M HCl).

Chemical Constituent	mmol/L	g/L
$NaHCO_3$	10.7079	0.8995
$KHCO_3$	0.3095	0.031
$MgSO_4 \cdot 7H_2O$	2.7031	0.6662
$CaSO_4 \cdot 2H_2O$	0.5608	0.0965
Na_2SO_4	1.7441	0.2477
NaCl	3.3006	0.1929

After the reduction phase of the experiment, sequestering agents were added to the batch reactors. Apatite-forming chemicals (trisodium citrate, calcium chloride, disodium phosphate, monosodium phosphate, and diammonium phosphate) were added at a stoichiometric ratio of 1.67 Ca/P (Moore et al. 2007; Szecsody et al. 2007, 2009). Calcite was formed by adding ammonium carbonate and calcium chloride (where the final concentrations for each chemical added was 0.05 M). NaOH was added at a final concentration of 0.05M. Batch reactors were left to equilibrate under anaerobic conditions for 1 week prior to removal from the chamber to maintain an oxygen-deficient environment. Post-equilibration, the reactors were opened to the atmosphere for a couple of minutes, resealed, and shaken gently to begin slow re-oxidation of the solutions. This process was repeated bi-weekly to simulate slow and periodic re-oxidation as will likely occur under field conditions. During this period, periodic sampling was performed (i.e., after 35, 49, and 154 days since the start of reduction) for each of the reactors to monitor aqueous phase contaminant concentrations.

2.4 Solid Phase Characterization

After 154 days, the sediments from batch reactors having the higher concentration of reducing agent (1% ZVI, 1% SMI, and 5% CPS), and associated controls, were analyzed. Briefly, reactor bottles were centrifuged, and the liquid decanted. Solid phase characterization of sediments included selective sequential extractions and X-ray absorption fine structure (XAFS).

Sediment samples were analyzed by sequential liquid extractions to quantify the total U and Tc concentration associated with distinct surface and mineral phases. For the extraction, 2 g of sediment was sequentially contacted with the following solvents: (1) synthetic perched water equilibrated with atmospheric oxygen, (2) 0.5 mol/L $Mg(NO_3)_2$ (pH 8), (3) 0.5M sodium acetate, (4) 0.26M glacial acetic acid (pH 5), and (5) 0.44M glacial acetic acid-0.1M $Ca(NO_3)_2$ (pH 2.3). For extractions 1-3, sediments were shaken for 50 minutes and then centrifuged for 15 minutes at 3000 rpm. For the fourth extraction, the sediments were shaken for 5 days, then centrifuged. Control sediments were further processed through extraction steps 5 and 6 using 0.1M ammonium oxalate–0.1M oxalic acid (shaken for 50 minutes) and 8M HNO_3 at 95°C (heat for 2 hours), respectively, to permit mass balance of U and Tc from the starting sediment. All of the aqueous samples were filtered with 0.45-µm PVDF filters and analyzed by inductively coupled plasma mass spectrometry and ion chromatography (with the exception for extractions 5 and 6).

For the XAFS analyses, selected samples were placed (100 mg) into a 10-mm x 3-mm polypropylene holder, encapsulated in Kapton, and packaged in additional Kapton/Mylar layers for analysis on the 20-BM-B beamline at the Advanced Photon Source (APS), located at Argonne National Laboratory (Lemont, Il USA). Uranium was measured using the L3-edge (17166 eV); due to the low concentration of Tc, XANES analysis was conducted (K-edge, 21044 eV). In addition, XANES analysis was acquired for Fe (K-edge, 7112 eV).

3.0 Results

3.1 Reductive Capacity

Reductive capacity measurements were performed for each of the reductants to normalize reductant concentrations and permit valid comparisons between experiments (Table 3.1). For the Fe- and Fe/S-based reductants (ZVI and SMI, respectively), the measured capacities were similar, with averaged values of 27.33 meq/g and 23.91 meq/g, respectively. The S-based reductant (CPS) had a lower capacity of 3.77 meq/g. Consequently, in these experiments ZVI and SMI were tested at 0.1 wt % and 1 wt %, while CPS was evaluated at 0.5 wt % and 5 wt % to yield equivalent reduction capacity across all experimental trials. Therefore, measured differences in the extent and rate of reductive immobilization of U and Tc were a function of the reactive mechanism(s) of each reductant, and not exclusively a mass dependent effect.

Table 3.1. Average measured and calculated reduction capacity for batch systems. The low concentration was 0.1 wt % for ZVI and SMI or 0.5 wt % for CPS, and the high concentration was set at 1 wt% for ZVI and SMI and 5 wt% for CPS.

Reductant	Measured Reductive Capacity (avg meq/g)	Low Reductive Capacity Reactor Concentration (meq)	High Reductive Capacity Reactor Concentration (meq)
ZVI	27.33 ± 0.85	2.83 ± 0.07	27.69 ± 0.39
SMI	23.91 ± 6.43	2.45 ± 0.11	23.95 ± 0.10
CPS	3.77 ± 0.11	2.40 ± 0.00	23.98 ± 0.00

3.2 Solution Phase Characterization from Batch Reactors

Remedy treatment effectiveness was evaluated (a) independently (i.e., as a single variable) and (b) in combination with chemical sequestration to determine the overall impact on aqueous phase contaminant immobilization. The percent U and Tc concentration removed from the aqueous phase was calculated over time. Both the solution and sediment controls were used to correct for variable background effects and daily instrument variation. This calculation was done by ratioing the measured concentration of the solution-sediment blanks and subtracting the ratio of the treated sample concentration to the initial spiked concentration.

3.2.1 Reduction-Only Mechanism

Table 3.2 defines the contaminant reduction baseline measurements for mechanistic chemical reactivity and effective reduction on individual contaminants per reductant. Experiments conducted with 0.1% ZVI resulted in the removal of 11% of the initial U and 95% of the initial Tc (Figure 3.1A,C); while treatments with 1% ZVI reduced the initial U and TC concentrations by 97% and 95%, respectively (Figure 3.1B,D). In comparison, 0.1% SMI (i.e., Fe and S reduction mechanism) immobilized 42% of the initial U and 95% of the initial Tc (Figure 3.2A,C). Reactors amended with 1% SMI reduced 97% of the initial U and 95% of the initial Tc (Figure 3.2B,D). For the S-only reduction mechanism, 0.5% CPS only reduced 0.3% of the initial U and 79% of the initial Tc (Figure 3.3A,C), while treatment with 5% CPS reduced 97% of the initial U and 95% of the initial Tc (Figure 3.3B,D).

Table 3.2. Percent removal of co-mingled U and Tc for the reduction only treatments after 154 days.

Analyte	wt % of Reductant	ZVI Fe Reduction	SMI Fe/S Reduction	CPS S Reduction
U238 (% removed)	Low	11.1 ± 10.0	42.2 ± 8.8	0.3 ± 7.7
	High	96.9 ± 0.0	96.7 ± 7.7	96.8 ± 7.7
Tc 99 (% removed)	Low	94.9 ± 0.0	94.9 ± 0.0	78.6 ± 1.4
	High	94.9 ± 0.0	94.9 ± 0.0	94.9 ± 0.0

3.2.2 Combined Reduction and Sequestration Mechanism

Table 3.3 provides the final percent removal of the co-mingled U and Tc from the solution phase when combining a reductant with a sequestering chemical. For reactors with 0.1% ZVI, when combined with a sequestering treatment the percent removal of U increased from 11% (reduction only) to 86% for apatite, 51% for calcite, and 96% for NaOH. Reactors amended with 1% ZVI did not show significant differences in U concentration when combined with the sequestering chemicals. Conversely, when Tc was treated with 0.1% ZVI, the aqueous concentration decreased from 100% reduction for reductant only to 77% with apatite, 97% for calcite, and 14% for NaOH. For samples treated with 1% ZVI, 100% of the Tc was removed from solution by reductant only, and decreased to 90% with apatite, while samples with NaOH only immobilized 65%. No significant change was detected in the percentage of Tc removed from the aqueous phase for the samples with 1% ZVI and calcite.

For comparison, after the reduction phase (28 days), the samples containing SMI had a 40% decrease of U in reactors with 0.1 wt% and 89% removal for reactors with 1 wt%; all the Tc was removed at the start of the sequestration step. Upon completion of this study, samples containing 0.1% SMI had a change in U reduction to 72% when combined with apatite, 44% when combined with calcite, and 93% when combined with NaOH. The measured Tc concentrations changed from complete reduction to 88% removed when combined with apatite, 96% removed when combined with calcite, and only 19% removed when combined with NaOH. Conversely, for samples containing 1% SMI, achieved near complete reduction of U>98% and Tc (>96%).

For reactors with the S reduction (i.e., CPS), upon addition of the sequestering chemicals, the removal for U was 4% in the reactors with 0.5 wt% of CPS and 95% for reactors with 5 wt% of CPS. The Tc removal was complete upon starting the second step with the sequestration chemicals. After completion of the 154-day experiment, in the low-concentration CPS reactors, the U removal increased to 96% when combined with apatite, 36% when combined with calcite, and was complete for treatment with the NaOH. For these reactors, the Tc decreased to 90% removal in the reactor with apatite, 62% in the calcite reactors, and 48% when combined with NaOH. In reactors containing 5 wt% CPS, there was a decrease in U removal only when combined with apatite; however, the U removal was complete for the treatments combined with calcite and NaOH. The measured removal of Tc was determined to be >94% in all cases.

Table 3.3. Percent U and Tc removed from the solution phase in batch reactors containing sequestration chemicals after test was completed (154 days).

Analyte	Sequestration-Reduction Batch Reaction	ZVI Fe Reduction	SMI Fe/S Reduction	CPS S Reduction	Sequestration Only
U238 (% Removed)	Apatite - Low	85.6 ± 16.1	72.1 ± 6.9	95.8 ± 5.3	74.0 ± 5.2
	Apatite - High	100.1 ± 5.2	101.1 ± 5.2	65.5 ± 7.1	
	Calcite - Low	50.8 ± 13.1	44.4 ± 7.9	35.8 ± 5.7	90.3 ± 5.2
	Calcite - High	101.2 ± 5.2	101.2 ± 5.2	101.7 ± 5.2	
	NaOH - Low	95.7 ± 5.2	93.3 ± 5.4	101.2 ± 5.2	97.3 ± 5.2
	NaOH - High	93.9 ± 5.2	98.0 ± 5.2	101.7 ± 5.2	
Tc 99 (% Removed)	Apatite - Low	76.8 ± 7.5	88.4 ± 3.0	90.1 ± 2.9	21.8 ± 5.5
	Apatite - High	89.5 ± 3.0	95.6 ± 2.5	93.6 ± 3.8	
	Calcite - Low	97.3 ± 2.8	96.1 ± 2.5	61.8 ± 3.2	0.7 ± 6.4
	Calcite - High	98.3 ± 0.0	98.3 ± 0.0	95.8 ± 2.4	
	NaOH- Low	13.6 ± 6.5	19.0 ± 6.0	47.6 ± 8.2	-1.9 ± 6.4
	NaOH - High	65.2 ± 3.9	98.3 ± 0.0	98.3 ± 0.0	

To understand the effects of combining a reductant with sequestration chemicals for the evaluation of remediation impacts of U and Tc over time, data was analyzed for temporal trends and to identify the susceptibility of sequestered contaminants to slow re-oxidation. Re-oxidation was initiated at day 35 days and allowed to proceed until day 154.

Quantification of the aqueous phase for reactors with the Fe-only reduction system, i.e., ZVI, showed a significant removal of U after the initial equilibration period. This change was measured to be greater than 80% in the case of apatite-ZVI (1%), calcite-ZVI (1%), and NaOH-ZVI (both 0.1% and 1%) (Figure 3.1A,B), where removal ultimately reached > 96% at the end of the experiment. Experiments containing 0.1% ZVI and apatite had an initial reduction of the U content from the perched water to 65% during the equilibration period and ending around 86% removed after 154 days (Figure 3.1A). For the 0.1% ZVI and calcite treatments, the U content that was removed from the perched water increased from 12% (pre-addition of the calcite forming chemicals) to 43% after the equilibration period without any significant change upon completion of the test (Figure 3.1A). In fact, the difference is within measurement error (i.e. analytical) compounded with the standard deviation between replicates and therefore is statistically insignificant. The measured aqueous phase results did not show significant remobilization of U after the oxic conditions were reintroduced for all experiments conducted with the chemical sequestration agents (i.e., calcite, apatite, and NaOH), confirming limited U re-mobilization even under oxic conditions.

Technetium was completely removed from the aqueous phase by both ZVI dosages (0.1% and 1.0%) prior to adding the sequestration chemicals; therefore, observed changes in the %Tc removed can be associated with some slight re-oxidation of the immobilized Tc during the secondary phase. In combination with the apatite treatments, there was an initial drop in the percent of Tc removed to ~85% for both the 0.1% and 1% ZVI doses after the initial equilibration period. During the re-oxidation phase, the percent of Tc removed changed to 77% for the 0.1% ZVI and 90% for the 1% ZVI treatments (Figure 3.1C,D). For the calcite treatments, the measured removal did not see significant changes between the addition of the calcite-forming solutions through re-oxidation. The measured removal for both ZVI concentrations ranged from 91% under anaerobic conditions to 98% under aerobic conditions (Figure 3.1C,D). The largest change in Tc concentration was observed for the samples that underwent mineral dissolution, where the concentration of reduced Tc after the equilibration period was 91% for both doses of reductant. However, the concentration then dropped to 14% Tc removed for the 0.1% treatment and

65% Tc removed for the 1% treatment (Figure 3.1C,D). For the sequestration-only reactors (Figure 3.1C,D), specifically calcite and NaOH, there was a limited impact of Tc uptake via either co-precipitation or incorporation mechanisms; however, apatite removed about 22% of the total TcO_4^- under oxic conditions.

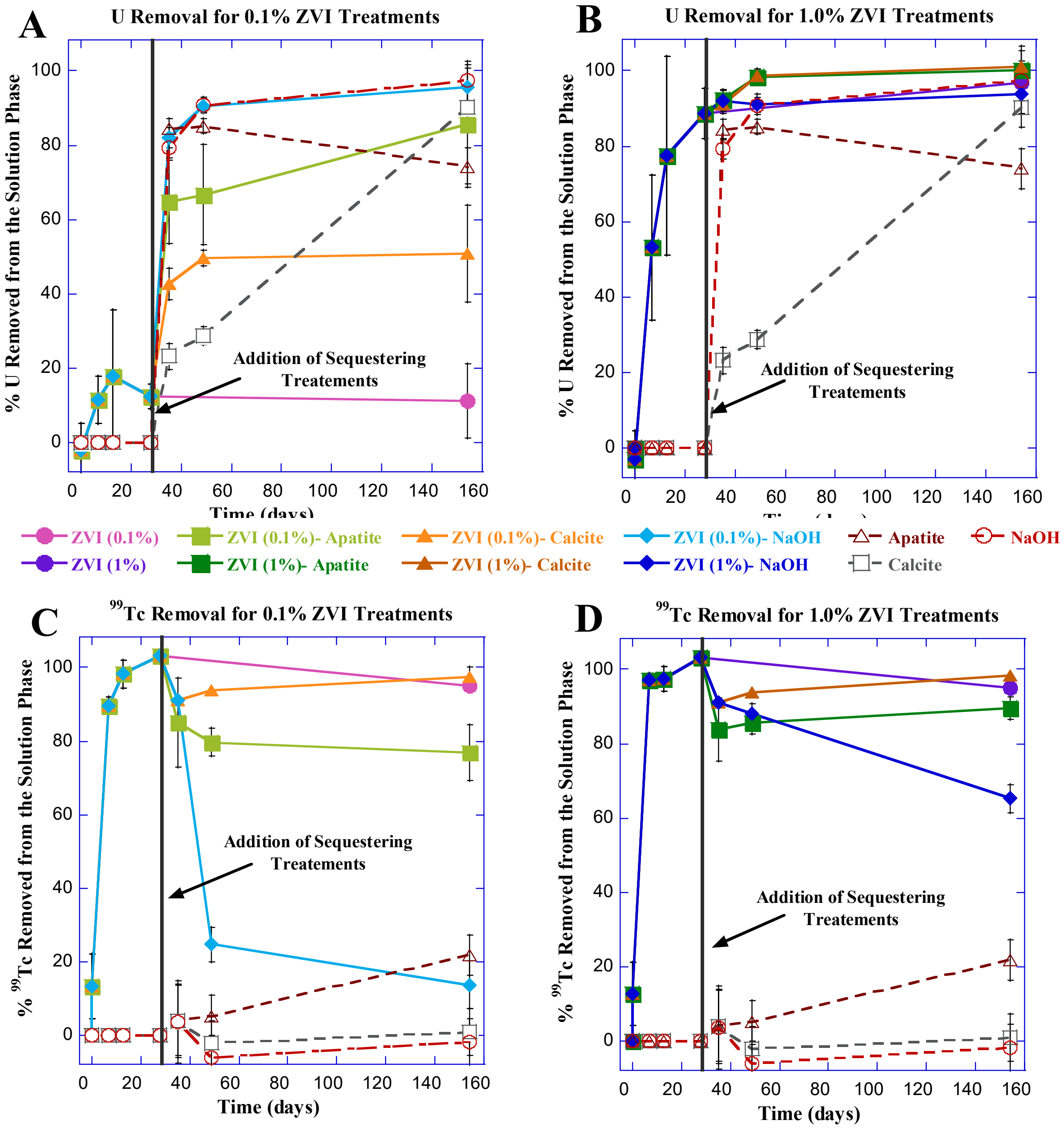

Figure 3.1. Effects of ZVI reduction on U and Tc in combination with sequestration chemicals (apatite, calcite, or NaOH). The above figures represent (A) 0.1% ZVI treatments and controls for U; (B) 1% ZVI treatments and controls for U; (C) 0.1% ZVI treatments and controls for Tc; and (D) 1.0 % ZVI treatments and controls for Tc.

As a comparison to the Fe-only system, SMI represents the mixed Fe/S reduction mechanism, shown in the batch reactor schematic (Figure 2.1). For all 1% SMI combined treatments, during the initial equilibration period there was no significant change in concentration of percent U removed; values ranged from 89% prior to adding sequestering chemicals to 90-92% post equilibration period for all treatments. During the re-oxidation phase, the values increased to >98% removed (Figure 3.2B). For the 0.1% SMI, the U removed changed from 40% prior to adding the sequestering chemicals to 70% for apatite, 52% for calcite, and 76% for NaOH during the equilibration phase. At the completion of the test, post re-oxidation, the U removed for each of these treatments was 72% for apatite, 44% for calcite, and 93% for NaOH (Figure 3.2A).

Prior to adding the sequestering chemicals, all aqueous TcO_4^- in this system was removed for both the 0.1% and 1% SMI experiments. For the experiments containing 0.1% SMI (Figure 3.2C), there was an initial decrease from complete reduction to about 87-91% of the Tc being removed. After the tests were exposed to oxygen, the Tc removal changed to 88% for apatite, 96% for calcite, and 19% for NaOH. For the reactors with 1% SMI, the range of Tc removal during the initial equilibration period was the same as the 0.1% SMI test. However, during the re-oxidation step, the Tc removal increased to >96% for all treatments (Figure 3.2D).

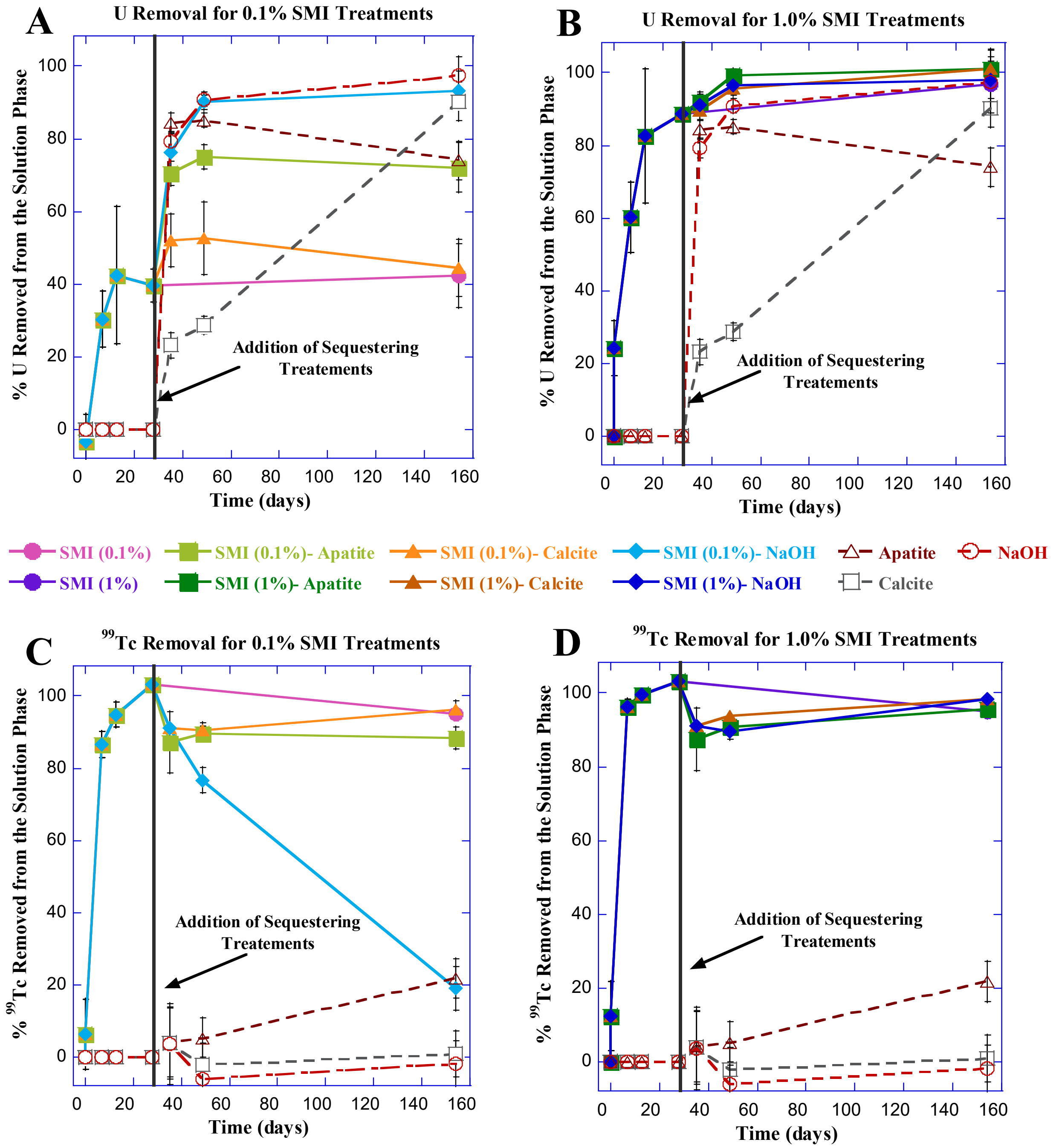

Figure 3.2. Effects of SMI reduction on U and Tc in combination with sequestration chemicals (apatite, calcite, or NaOH). The figures show (A) 0.1% SMI treatments and controls for U; (B) 1% SMI treatments and controls for U; (C) 0.1% SMI treatments and controls for Tc; and (D) 1.0 % SMI treatments and controls for Tc.

Lastly, CPS (Figure 3.3) was examined as the sulfur-only reducing system as defined in the reactor scheme shown in Figure 2.1. In the experiments conducted with a lower concentration of CPS (0.5%), Figure 3.3A, the removal of aqueous U was low (4%) prior to adding the sequestering chemicals. After the initial anerobic equilibration period (7 days) with the various treatments, the U removal increased to 91% with apatite, 34% with calcite, and 84% by mineral dissolution. After re-oxidation, there were no significant increases for the apatite and calcite treatments, where the final removal was 96% and 36%, respectively. However, the treatments that were in combination with mineral dissolution had complete removal of U from the aqueous phase. In comparison to the reactors containing 5% CPS, U removal was at 95% for all experiments at the start of phase two (Figure 3.3B). During the initial equilibration period, there was no significant change in U reduction for any of the treatments. After addition of the sequestration chemicals, the U was completely removed from the aqueous phase in the reactors containing calcite or NaOH. However, when apatite was introduced, the reduced U concentration decreased from 95% to 66% by the end of the 154 days.

When S was used as the reduction mechanism for the initial TcO_4^- anion, it was observed that all of the Tc was removed for both the 0.5% and 5% CPS reactors prior to starting the sequestration step (Figure 3.3D). Upon addition of the chemicals, Tc appeared to slightly resolubilize in all of the 0.5% CPS reactors. For the apatite treatment, the removed Tc was 85% after the equilibration period and then increased to 90% by 154 days, most likely a mechanism of co-precipitation. In the presence of calcite, Tc removal dropped to 87% during the anoxic equilibration period, while after exposure to atmospheric oxygen the Tc removal dropped to 62% by day 154. For the mineral dissolution treatment, the initial concentration was at 89% reduction post equilibration, after which the removal trend was similar to the calcite treatment, leaving only 48% still reduced by day 154. Even under anoxic conditions, the 0.5% CPS treatment independently remobilized 79% of Tc by the end of the experiment (154 days). For the 5% CPS treatments (Figure 3.3E), the small amount of re-oxidization may have occurred during the addition of the sequestering treatments. The percent Tc removed for all treatments initially dropped to 91% from 95% during the anoxic equilibration period. However, the system rebounded even under exposure to atmospheric oxygen, where the final percentages of Tc removal from the aqueous phase were 94%, 96%, and 98% for apatite, calcite, and NaOH, respectively.

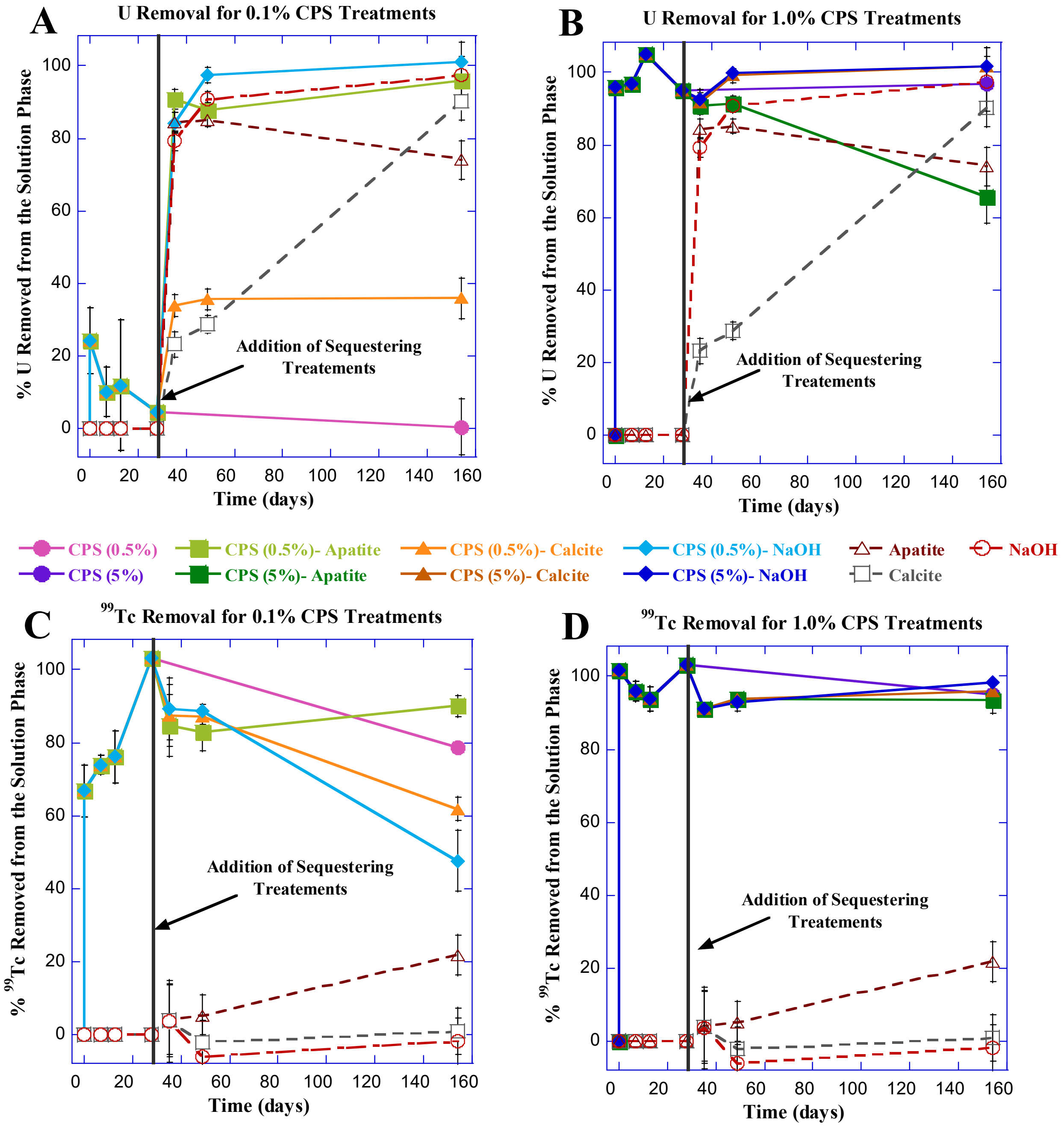

Figure 3.3. Effects of CPS reduction on U and Tc in combination with sequestration chemicals (apatite, calcite, or NaOH). Figures above depict (A) 0.1% CPS treatments and controls for U; (B) 1% CPS treatments and controls for U; (C) 0.1% CPS treatments and controls for Tc; and (D) 1.0 % CPS treatments and controls for Tc.

3.3 Post-Experimental Solid Phase Characterization

Sequential Extractions. Upon completion of the 154-day tests, samples with the highest reductant concentrations were selected for sediment characterization to quantify contaminant mass residing on mineral surfaces and precipitate phases formed during experimentation.

Table 3.4 provides the results describing the recovery of U and Tc by sequential extraction of sediments from the reactors with the higher reduction doses. The first four selective extractions are expected to be the most site relevant, signifying the contaminant fraction most susceptible to dissolution and/or oxidation release under realistic field conditions. For comparison, contaminant concentration associated with the sediment phases was calculated by difference based on results collected in the aqueous phase.

Table 3.4. Calculated sequential extraction results for U and Tc.

Sample	Selectively Extracted Tc^{99} (µg/g)	Tc^{99} Reduce from Solution (µg/g)	Total Tc^{99} Extracted (%)	Selectively Extracted U (µg/g)	U Reduced from Solution (µg/g)	Total U Extracted (%)
ZVI (1%)	0.027 ± 0.004	1.780 ± 0.000	1.5 ± 0.2	317.74 ± 75.53	1455.00 ± 0.000	21.8 ± 5.2
ZVI (1%) - Apatite	0.093 ± 0.020	1.628 ± 0.030	5.7 ± 1.4	298.41 ± 26.67	1433.70 ± 4.16	20.8 ± 1.8
ZVI (1%) - Calcite	0.028 ± 0.018	1.780 ± 0.000	1.6 ± 1.0	475.27 ± 213.54	1447.62 ± 0.51	32.8 ± 14.7
ZVI (1%) - NaOH	0.031 ± 0.000	1.201 ± 0.048	2.6 ± 0.1	366.03 ± 8.71	1351.54 ± 3.23	27.1 ± 0.7
SMI (1%)	0.024 ± 0.001	1.780 ± 0.000	1.3 ± 0.0	85.93 ± 3.40	1452.31 ± 1.46	5.9 ± 0.2
SMI (1%) - Apatite	0.033 ± 0.008	1.733 ± 0.008	1.9 ± 0.4	142.76 ± 25.59	1446.53 ± 0.45	9.9 ± 1.8
SMI (1%) - Calcite	0.005 ± 0.001	1.780 ± 0.000	0.3 ± 0.1	122.71 ± 77.44	1448.03 ± 0.88	8.5 ± 5.3
SMI (1%) - NaOH	0.020 ± 0.001	1.780 ± 0.000	1.1 ± 0.1	278.44 ± 18.58	1406.13 ± 3.53	19.8 ± 1.4
CPS (1%)	0.015 ± 0.003	1.780 ± 0.000	0.9 ± 0.2	909.25 ± 42.23	1454.10 ± 0.14	62.5 ± 2.9
CPS (1%) - Apatite	0.012 ± 0.001	1.699 ± 0.053	0.7 ± 0.1	390.86 ± 15.92	986.57 ± 79.27	39.7 ± 1.6
CPS (1%) - Calcite	0.007 ± 0.001	1.737 ± 0.000	0.4 ± 0.0	765.66 ± 117.96	1454.25 ± 0.18	52.7 ± 8.1
CPS (1%) - NaOH	0.037 ± 0.010	1.780 ± 0.000	2.1 ± 0.6	804.59 ± 16.42	1454.93 ± 0.00	55.3 ± 1.1
Apatite	0.128 ± 0.037	0.421 ± 0.040	30.2 ± 6.0	182.84 ± 8.90	1084.27 ± 3.56	16.9 ± 0.8
Calcite	0.055 ± 0.000	0.044 ± 0.037	194.1 ± 164.6	245.80 ± 0.73	1301.43 ± 7.97	18.9 ±0.2
NaOH	0.055 ± 0.003	0.002 ± 0.033	-12.2 ± 333.9	859.39 ± 18.62	1395.32 ± 2.35	61.6 ± 1.2

XANES Analyses. Select samples were analyzed using the 20-ID-BM Beamline at the APS to determine oxidation state and speciation changes in contaminants and other elements of interest found in the sediments collected from the batch reactors post-treatment. Based on reduction of contaminants from the solution phase, combination treatment samples analyzed at APS included: ZVI-Calcite, ZVI-NaOH, SMI-Apatite, SMI-Calcite, SMI-NaOH, CPS-Apatite, CPS-Calcite. These samples were analyzed for U, Fe, and Tc (if detectable). Of the samples analyzed, ZVI and SMI had Fe added as part of the reduction step; however, for the CPS samples, the measured Fe was sourced from the mineral phases already present in the sediment. The determined Fe speciation in these natural Fe sources are expected to be different when compared to the ZVI and SMI samples. Initial observations of the U speciation in all samples indicate mostly U(VI), except for SMI-calcite, which is mostly U(IV), when compared to UO_2 and UO_3 standards (Figure 3.4).

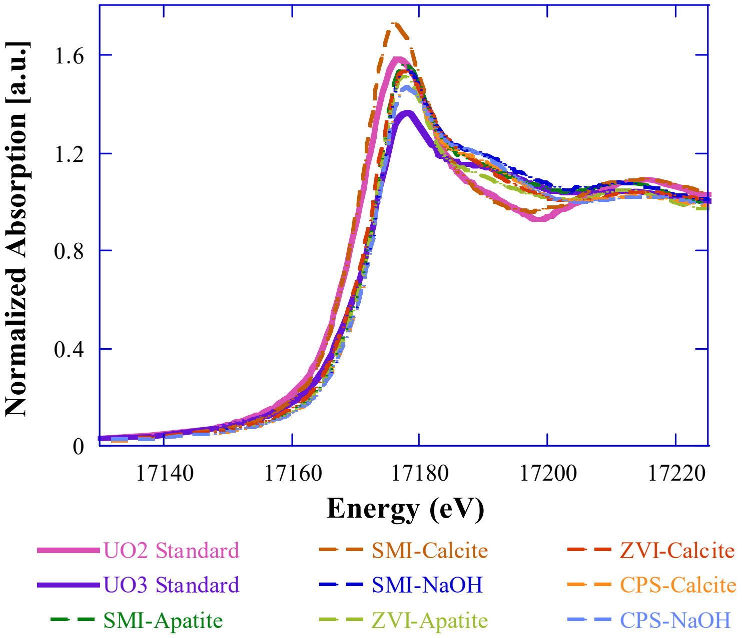

Figure 3.4. Measured U speciation for select samples as compared to known U(IV) standard [UO_2] vs. U(VI)standard as [UO_3]. Measured U edge values were collected using the L3-edge at 17166 eV.

To quantitatively determine the fraction of U(IV) and U(VI) species in each sample, a linear combination fit (LCF) (Appendix A, Figure A.1.) is used and depicts how the measured speciation for all the samples, excluding SMI-Calcite, is not 100% U(IV). In fact, there is a mixture of U(IV)/(VI) speciation for the other combination of treatments. The speciation proportions of U(IV)/(VI) are found in Table 3.5. Knowledge of the ratio of U(IV)/U(VI) will be used to define the various pathways for long-term remediation of U via the various combinations of treatments.

Table 3.5. LCF ratio of UO_2 and UO_3 for all treatments.

	ZVI-Apatite	ZVI-Calcite	SMI-Apatite	SMI-Calcite	SMI-NaOH	CPS-Calcite	CPS-NaOH
UO_2	0.423	0.586	0.431	1	0.297	0.315	0.327
UO_3	0.565	0.424	0.59	0.025	0.734	0.683	0.676
Sum	0.988	1.01	1.021	1.025	1.031	0.998	1.003

Since the Tc concentration was spiked as <1ppm TcO_4^- in the aqueous phase, the K-edge at 21044 eV was difficult to find with only three samples having a detection from this set when analyzed at ANL. Samples where the speciation can be determined by XANES analysis included SMI-Apatite, SMI-Calcite, and ZVI-Calcite (Figure 3.5). Collected data shows Tc as the reduced Tc(IV) complex rather than initial pertechnetate anion (TcO_4^-). The data suggests the combined reduction and sequestration approach has prevented re-oxidation of Tc(IV) to TcO_4^-. Positive identification of the Tc(IV) complex(es) formed was not feasible because of the low concentrations used in these experiments; the detection limit for Tc is around 1 ppm.

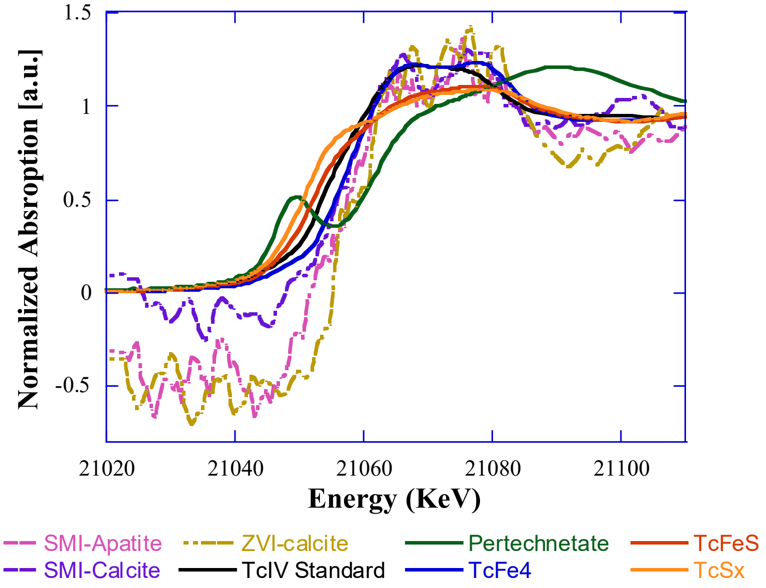

Figure 3.5. Measure Tc edge (K-edge, 21044 eV) for select samples using the two-step approach. Speciation of Tc in select samples is compared to various known standards or complexes.

XANES measurements identified the presence of mixed Fe species in all treatments. The measured Fe sources originate from either the reduction constituent or from sources within the sediments. In Appendix A, Figure A.2 compares each of the LCF corrected Fe XANES data. To compare the samples and determine ratios of various mineral formations, six standards were chosen: more specifically, magnetite (Fe_3O_4), hematite (Fe_2O_3), wustite (FeO), $FeCO_3$, $FePO_4$, and Aegirine ($NaFeSi_2O_6$). Each of these standards represents potential species based on the reduction and sequestration mechanism, in addition to mineral forms from the sediments post-treatment. Of the six standards used for evaluation of Fe speciation, $FeCO_3$ and $FePO_4$ did not significantly contribute to the overall fit (fraction $< 2\sigma$); therefore, the final table of calculated percentages for each type does not include these two minerals (Table 3.6). Measured Fe in the system was not only through addition since some of the treatments received no Fe reduction chemical. Therefore, the Fe speciation reported in Table 3.6 also represents systems where Fe from the sediments was altered, providing a secondary reduction system for co-mingled contaminants.

Table 3.6. LCF Fe speciation based on six standards for all samples.

	SMI-Apatite	SMI-Calcite	SMI-NaOH	ZVI-Apatite	ZVI-Calcite	CPS-Calcite	CPS-NaOH
Aegirine ($NaFeSi_2O_6$)	0.914 ± 0.015	0.868 ± 0.013	0.176 ± 0.102	0.193 ± 0.079	0.815 ± 0.008	0.972 ± 0.125	0.664 ± 0.089
Wustite (FeO)	0.061 ± 0.016	0.109 ± 0.014		0.14 ± 0.039	0.167 ± 0.009		
Magnetite (Fe_3O_4)			0.428 ± 0.032	0.361 ± 0.047			
Hematite (Fe_2O_3)			0.384 ± 0.126	0.299 ± 0.099		0 ± 0.132	0.312 ± 0.094
Sum	0.975	0.977	0.988	0.993	0.982	0.972	0.976

4.0 Discussion

The goal of this work was to investigate and evaluate the effectiveness of a two-step subsurface remediation approach to 1) reductively immobilize contaminants in-situ and 2) coat or encapsulate contaminant in low solubility mineral phases that slow or prevent oxidative remobilization once natural (oxic) conditions reestablish in the system. The reductants used in this study have been subject to numerous investigations and have deployed successfully in field-scale permeable reactive barriers (PRB) to remove contaminants like U, Tc, Cr, As, Pb, Mo, Ni, Hg, PO_4, Se, and VOCs (ITRC 2005; Lawter et al. 2018; Szecsody et al. 2004; SGW-38255 2009). Secondarily, this work was conducted to identify the potential for contaminant remobilization. For example, oxic conditions naturally exist in the perched aquifer in the deep vadose zone at the Hanford Site, which is common to many groundwater systems. With the addition of a reductant, independent of a sequestering agent, the reducing environment created in these systems would eventually oxidize and re-mobilize previously reduced contaminants.

For the Fe only (i.e., ZVI) based reductant, reaction with metals and metalloids occurs primarily through reductive precipitation or as a co-precipitant with iron oxyhydroxides that form on the surfaces of the ZVI . The secondary mechanism of contaminant immobilization is through sorption onto iron oxyhydroxides formed during the oxidation of the ZVI (Tratnyek et al. 2015). For the ZVI reduction only system, aqueous phase analysis of the batch experiments suggests that even under continued reducing conditions, Tc can oxidize and re-mobilize in the aqueous phase. Solid phase sequential extractions identified for both concentrations of ZVI tested that only 1.5% to 5.8% of the immobilized Tc is potentially oxidizable, and ~20-22% of the U was extractable.

To identify the importance of a Fe/S reduction pathway, data collected from the aqueous phase shows a higher reduction of U for the 0.1% SMI treatment relative to the 0.1% ZVI. However, results for the 1% concentration are similar between SMI and ZVI. Conversely, the sediment phase characterization suggested limited re-oxidation potential when SMI was used. For Tc there was only 1.3% extractable, and for U, 5.9% was extractable for oxidation sensitive phases. These results suggest that SMI is a more efficient reductant for U and Tc than ZVI under the tested conditions.

By comparison to ZVI and SMI, CPS (CaS_x, where x ranges from 3 to 7) is an S only reduction mechanism. For this two-step approach study, when CPS was added there was an immediate and complete reduction of Tc prior to starting the sequestration step. Uranium reduction with CPS was immediate for the experiments conducted with the 5% CPS solution but had similar results to ZVI/SMI for the 0.5% CPS solution. Data collected from the sediment phase characterization suggests that 0.9% of the Tc and 62.5% of the U may undergo re-oxidation. Solid phase characterization data shows how important the formation of Tc_2S_x phases is to the overall reduction and immobilization of Tc from aqueous systems (Szecsody et al. 2015; Wen et al. 2018).

When the reducing agent applications are combined with the application of a sequestration technique (second step), such as the addition of apatite or calcite forming solutions or addition of a strong base to promote mineral dissolution and reprecipitation, there is further removal and stabilization of U and Tc. Each of these combined techniques has been evaluated and results are summarized in Table 3.2 and Table 3.3. However, the mechanism for further reduction of co-mingled contaminants may vary between incorporation, co-precipitation, new mineral formation, or the formation of mineral coatings on precipitated contaminant mineral phases.

Apatite [$Ca_5(PO_4)_3(F,OH,Cl)$] is a relatively insoluble mineral that can be used to sequester metal and radionuclide contaminants through co-precipitation and adsorption. Phosphate in various forms has been previously tested at the Hanford site to sequester selected radionuclides like U and ^{90}Sr (Fritz et al 2011; SGW-59614, Rev. 0; SGW-56970, Rev. 0; SGW-47062, Rev. 0; Szecsody et al. 2010a; Vermeul et al.

2009; Vermeul et al. 2010; Wellman et al. 2011). When apatite was combined with a reductant, there was an increase in reduction of aqueous U following the mechanism of co-precipitation and/or adsorption as previously defined. Solid phase characterization suggests that SMI combined with apatite is one of the best combined approaches for successful stabilization of reduced U and Tc. At the end of the 154-day experiment, 100% of U was removed from solution and only 9.9% was extractable from the solid phase. XANES analysis showed that the U phases present under these conditions are a mixture of U(IV)/U(VI), suggesting that U had precipitated as U(IV) species and had likely undergone some re-oxidation and adsorbed to the apatite mineral. However, the sequestration mechanism limits the re-oxidation of U. Similar results were found for Tc, where only 1.9% was extractable with a total removal from the solution phase of 96% in the 1% SMI-apatite samples.

Another method of in-situ mineral formation tested in this study was by calcite forming solutions. Similar work has been previously tested in combination with ZVI or SMI (Lawter et al. 2018). The combined SMI with calcite approach was highly effective for both U and Tc reduction from the aqueous phase. Complete removal of U and Tc was observed in the aqueous phase, and only 0.3% (Tc) and 8.5% (U) was readily extractable from the solid phase. Therefore, there does not appear to be re-oxidation pathways for either contaminant. XANES analysis of U for the SMI-calcite treatment shows this is the only sample characterized to have U(IV) and no U(VI), providing evidence that calcite has prevented any oxidation of the reduced U.

As an alternative to in situ mineral formation, alkaline treatments have been tested at Hanford as a stand-alone treatment mechanism (Emerson et al. 2017, 2018; Szecsody et al. 2010b, 2012, 2013; Zhong et al. 2015). The sequential reduction and sequestration approach with SMI-NaOH and CPS-NaOH was less effective than other reductant-sequestration combinations. Characterization of the solid phase SMI-NaOH showed limited extractable Tc and U, where the removal of these constituents from the aqueous phase was low, 1.1% and 19.8% respectively. Examination of the solid phase extraction for the CPS-NaOH combined treatment were 0.4% and 55.3%. XANES analysis of these two treatment pathways shows similar ratios of U(IV)/(VI) present.

5.0 Conclusions

In these batch reactors the SMI application in combination with apatite or calcite precipitating minerals was shown to be the most effective method for removing both U and Tc from the aqueous phase. No interferences were noted for U and Tc co-location during both the reduction and sequestration steps. In addition, evaluation of the various combinations of reductants and sequestering agents has shown that different mechanisms drive the removal of COCs from the aqueous phase, e.g., co-precipitation, mineral dissolution/re-precipitation, incorporation, and mineral coatings. To identify the potential for re-oxidation and subsequent re-mobilization, oxidizing conditions were introduced and demonstrated that when the low concentration of reductant was used, oxidation of U and Tc was more likely. Other examples include combinations using the high concentration of the reductant like ZVI-NaOH for U or CPS-Apatite for Tc. However, this impact can be minimized with the formation of mineral coatings with calcite or apatite, or via incorporation and/or co-precipitation. More specifically, excellent contaminant stabilization was observed when these sequestering treatments were combined with the high concentration of a reductant like SMI.

Further assessment of long-term contaminant stability and mass balance needs to be carefully evaluated. In addition, characterization of the impact microbial communities can play on reduction-sequestration effects needs to be evaluated. Column studies can be used to examine the impact of this two-step approach to mobilization via simulated groundwater movements. In general, the largest impact to scaling-up this approach would be the delivery mechanism for SMI or nano SMI (nSMI). Other field studies using this approach have used emulsification or a modified reductant as a delivery system; however, this study has not examined the effects of these mechanisms on reduction of co-mingled contaminants (Fan et al. 2015, ITRC 2005). Overall, this two-step approach can be considered as a remediation strategy for a variety of contaminants in systems with slow-moving water.

6.0 Quality Assurance

This work was performed in accordance with the Pacific Northwest National Laboratory (PNNL) Nuclear Quality Assurance Program (NQAP). The NQAP complies with the United States Department of Energy Order 414.1D, *Quality Assurance*. The NQAP uses NQA-1-2012, *Quality Assurance Requirements for Nuclear Facility Application* as its consensus standard and NQA-1-2012 Subpart 4.2.1 as the basis for its graded approach to quality.

This work emphasized acquiring new theoretical or experimental knowledge. The information associated with this report should not be used as design input or operating parameters without additional qualification.

7.0 References

Angus MJ and FP Glasser. 1985. The chemical environment in cement matrices. MRS Online Proceedings. Cambridge University Press. 50:547-556.

Bagwell CE, AR Lawter, KJ Cantrell, CF Brown. 2018. Evaluation of Central Plateau Remediation Alternatives: Interim Status Report: FY18. PNNL-28055, Richland, WA.

Campbell KM, RK Kukkadapu, NP Qafoku, AD Peacock, E Lesher, KH Williams, JR Bargar, MJ Wilkins, LA Figueroa, J Ranville, J Davis, and PE Long. 2012. Geochemical, mineralogical and microbiological characteristics of sediment from a naturally reduced zone in a uranium-contaminated aquifer. Applied Geochemistry 27(8):1499-1511. doi:10.1016/j.apgeochem.2012.04.013

DOE/RL-2016-69, Rev. 0. Calendar Year 2016 Annual Summary Report for the 200-ZP-1 and 200-DV-1 Operable Unit Pump-and-Treat Operations. U.S. Department of Energy Richland Operations Office, Richland, WA.

Fan D, GO Johnson, PG Tratnyek, RL Johnson. 2016. Sulfidation of Nano Zerovalent Iron (nZVI) for Improved Selectivity During In-situ Chemical Reduction (ISCR). Environ. Sci. Technol. 50(17):9558-9565.

Fan D, RP Anitori, BM Tebo, PG Tratnyek. 2013. Reductive Sequestering of Pertechnetate (99TcO4-) by Nano Zerovalent Iron (nZVI) Transformed by Abiotic Sulfide. Environ. Sci. Technol. 47: 5302-5310.

Fan D, RP Anitori, BM Tebo, PG Tratnyek. 2014. Oxidative Remobilization of Techetium Sequestered by Sulfide-Transformed Nano Zerovalent Iron. Environ. Sci. Technol. 48: 7409-7417.

Fan D, S Chen, RL Johnson, PG Tratnyek, PG. 2015. Field Deployable Chemical Redox Probe for Quantitative Characterization of Carboxymethylcellulose Modified Nano Zerovalent Iron. Environ. Sci. Technol. 49, 10589−10597.

Icenhower JP, NP Qafoku, WJ Martin and JM Zachara. 2008. The geochemistry of technetium: A summary of the behavior of an artificial element in the natural environment. PNNL-18139, Pacific Northwest National Laboratory, Richland, WA.

Ilton E, NP Qafoku, C Liu, DA Moore, JP Zachara. 2008. Advective dissolution of uranyl silicates from the BX-102 sediments. Environ. Sci. Technol. 42: 1565-1571.

Kaplan DI, T Hang, SE Aleman. 2005. Westinghouse Savannah River Company WSRC-RP-2005-01674 Rev. 0.

Lawter AR, WL Garcia RK Kukkadapu, O Oafoku, ME Bowden, SA Saslow, NP Qafoku. 2018. Technetium and iodine aqueous species immobilization and transformations in the presence of strong reductants and calcite-forming solutions: Remedial action implications. Sci. Total Environ. 636: 588-595.

Liu Y, C Liu, RK Kukkadapu, JP McKinley, J Zachara, AE Plymale, MD Miller, T Varga, CT Resch, C.T. 2015. 99Tc(VII) Retardation, Reduction, and Redox Rate Scaling in Natrually Reduced Sediments. Environ. Sci. Technol. 49:13403-13412.

Moore R, J Szecsody, M Truex, K Kelean, R Bontchev, C Ainsworth. 2007. Formation of nanosize apatite crystals in sediments for contaminant and stabilization of contaminants, Environmental

Applications of Nanomaterials, Synthesis, Sorbents, and Sensors. Eds G. Fryxell and G. Cao, Imperial College Press. p 89-109.

N'Guessan AL, HS Moon, AD Peacock, H Tan, M Sinha, PE Long, and PR Jaffe. 2010. Postbiostimulation microbial community structure changes that control the reoxidation of uranium. FEMS Microbiology Ecology 74(1), 184-195.

Oostrom M, MJ Truex, KC Carroll, GB Chronister. 2013. Perched-water analysis related to deep vadose zone contaminant transport and impact to groundwater. J. Hydrology 505:228-239.

Pearce CI, RJ Serne, SA Saslow, W Um, RM Asmussen, MD Miller, O Qafoku, MMV Snyder, CT Resch, KC Johnson, G Wang, SM Heald, JE Szecsody, JM Zachara, NP Qafoku, AE Plymale, VL Freedman. 2018. Characterizing technetium in subsurface sediments for contaminant remediation. ACS Earth and Space Chemistry 2(11):1145-1160.

Plymale AE, JK Fredrickson, JM Zachara, AC Dohnalkavoa, SM Heald, DA Moore, DW Kennedy, MJ Marshall, C Wang, CT Resch, P Nachimuthu. 2011. Competitive Reduction of Pertechnetate (99TcO4-) by Dissimilartory Metal Reducing Bacteria and Biogenic Fe(II). Environ. Sci. Technol. 45: 951-957.

Qafoku NP, PE Dresel, ES Ilton, JP McKinley, and CT Resch. 2010. Chromium transport in an acidic waste contaminated subsurface medium: The role of reduction. Chemosphere 81(11):1492-1500. doi:10.1016/j.chemosphere.2010.08.043

Saslow SA, AR Lawter, BN Gartman, F Zhang, MMV Snyder L Zhong, KJ Cantrell, CF Brown. 2018. Evaluation of Perched Water Post-Extraction Remedy Technologies: Interim Status Report. FY18. PNNL-28054, Richland, WA.

Szecsody JE, JS Fruchter, MD Williams, VR Vermeul, and DS Sklarew. 2004. In Situ Chemical Reduction of Aquifer Sediments: Enhancement of Reactive Iron Phases and TCE Dechlorination. Environ. Sci. Technol. 17:4656-4663.

Szecsody J, C Burns, R Moore, J Fruchter, V Vermeul, D Girvin, J Phillips, M Williams. 2007. Hanford 100N Area Apatite Emplacement: Laboratory Results of Ca-Citrate-PO4 Solution Injection and Sr-90 Immobilization in 100N Sediments, PNNL report. PNNL-16891.

Szecsody J, M Rockhold, M Oostrom, R Moore, C Burns, M Williams, L Zhong, J Fruchter, J McKinley, V Vermeul, M Covert, T Wietsma, A Breshears, B and Garcia. 2009. Sequestration of Sr-90 Subsurface Contamination in the Hanford 100-N Area by Surface Infiltration of a Ca-Citrate-Phosphate Solution. Pacific Northwest National Laboratories, PNNL-18303.

Szecsody JE, MJ Truex, L Zhong, NP Qafoku, MD Williams, JP McKinley, Z Wang, J Bargar, DK Faurie, CT Resch, and JL Phillips. 2010. Remediation of Uranium in the Hanford Vadose Zone Using Ammonia Gas: FY 2010 Laboratory-Scale Experiments. PNNL-20004, Richland, WA.

Szecsody JE, MJ Truex, L Zhong, TC Johnson, NP Qafoku, MD Williams, et al. 2012. Geochemical and geophysical changes during NH3 gas treatment of vadose zone sediments for uranium remediation. Vadose Zone J. 11(4). doi:10.2136/vzj2011.0158

Szecsody JE, MJ Truex, NP Qafoku, DM Wellman, T Resch, and L Zhong. 2013. Influence of acidic and alkaline co-contaminants on uranium migration in vadose zone sediments. J. Contam. Hydrol. 151:155–175. doi:10.1016/j.jconhyd.2013.05.009

Szecsody J, D Jansik. 2015. Technetium Reduction and Permanent Sequestering by Abiotic and Biotic Formation of Low-Solubility Sulfide Mineral Phases. ID: ER64806-1033401-0015142.

Szecsody JE, MJ Truex, L Zhong, JP McKinley, NP Qafoku, BD Lee, SD Saurey. 2015. Remediation of Technetium in Vadose Zone Sediments Using Ammonia and Hydrogen Sulfide Gases. Vadose Zone J. 14 (7): vzj2014.09.0134. doi:

Szecsody JE, BD Lee, MJ Truex, CE Strickland, JJ Moran, MMV Snyder, AR Lawter, CT Resch, BN Gartman, L Zhong, MK Nims, DL Saunders, BD Williams, JA Horner, II Leavy, SR Baum, BB Christiansen, RE Clayton, EM McElroy, and D Appriou. 2017. Geochemical, Microbial, and Physical Characterization of 200-DV-1 Operable Unit Cores from Boreholes C9552, C9487, and C9488, Hanford Site Central Plateau. PNNL-26266, Pacific Northwest National Laboratory, Richland, WA.

Szecsody JE, CI Pearce, KJ Cantrell, NP Qafoku, G Wang, EC Gillispie, AR Lawter et al. 2018. Evaluation of remediation technologies for iodine-129: FY18 bench scale results. Technical Report. PNNL-28064. Richland, WA, Pacific Northwest National Laboratory.

Thomson NR, MJ Fraser, C Lamarche, JF Barker, and SP Forsey. 2008. Rebound of a coal tar creosote plume following partial source zone treatment with permanganate. Journal of Contaminant Hydrology 102(1):154-171. doi:https://doi.org/10.1016/j.jconhyd.2008.07.001.

Tratnyek PG, BM Tebo, D Fan, R Anitori, J Szecsody, D Jansik. 2015. Technetium Reduction and Permanent Sequestration by Abiotic and Biotic Formation of Low-Solubility Sulfide Mineral Phases. Technical Report. ER64806-1033401-0015142

Truex MJ, JE Szecsody, L Zhong, and NP Qafoku. 2014. Gas-Phase Treatment of Technetium in the Vadose Zone at the Hanford Site Central Plateau. PNNL-23665, Pacific Northwest National Laboratory, Richland, WA.

Wellman DM, JM Zachara, C Liu, NP Qafoku, SC Smith, and SW Forrester. 2008. Advective Desorption of Uranium (VI) from Contaminated Hanford Vadose Zone Sediments under Saturated and Unsaturated Conditions. Vadoze Zone Journal. 7(4): 1144–1159. doi:10.2136/vzj2007.0166

Wen H, Z Pan, D Giammar, L Li. 2018. Enhanced Uranium Immobilization by Phosphate Amendment under Variable Goechemical and Flow Conditions: Insights from Reactive transport Modeling. Environ. Sci. Technol. 52(10):5841-5850.

Wu WM, J Carley, J Luo, MA Ginder-Vogel, E Cardenas, MB Leigh, C Hwang, SD Kelly, C Ruan, L Wu, J Van Nostrand, T Gentry, K Lowe, T Mehlhorn, S Carroll, W Luo, MW Fields, B Gu, D Watson, KM Kemner, T Marsh, J Tiedje, J Zhou, S Fendorf, PK Kitanidis, PM Jardine, CS Criddle. 2007. In situ bioreduction of uranium(VI) to submicromolar levels and reoxidation by dissolved oxygen. Environmental Science and Technology 41, 16: 5716-5723.

Zhong L, JE Szecsody, MJ Truex, MD Williams, and Y Liu. 2015. Ammonia gas transport and interaction with sediment and pore water under vadose zone conditions. J. Hazard. Mater. 289118–129. doi:10.1016/j.jhazmat.2015.02.025

Appendix A – XANES

XANES spectra were collected at APS Beamline 20-BM-B using a Si(111) monochromator under ambient conditions. For analysis of the U L3-edge (17166 eV) a Zr foil was used as the reference. For analysis, UO_3 and UO_2 standards were measured prior data collection for the samples. Data collected for the samples was obtained with a range of 200 eV below the edge and ~850eV above the edge. For all measurements, the data was collected at 20eV below and 40 eV above the edge, with a step size of 0.5 eV increments and 10 eV increments for the pre-edge. For the standards, SMI-apatite, SMI-calcite, SMI-NaOH data was collected from $1 \leq k \leq 14.985$ with 0.05 eV increments. The rest of the samples (ZVI-Apatite, ZVI-calcite, CPS-Calcite, and CPS-NaOH) data was collected from $1 \leq k \leq 7.976$ with 0.05 eV increments.

Due to the low concentration of Tc XANES, analysis was harder to collect at the K-edge, (21044 eV). Data collected for the Tc measurements had a range of 200 eV below the edge and ~230eV above the edge. For all measurements, data was collected at 20 eV below and 40 eV above the edge with a step size of 0.5 eV and increments for the pre-edge was 10eV.

In addition, XANES analysis was acquired for Fe (K-edge, 7112 eV), data collected for the samples was obtained with a range of 150 eV below the edge and ~250eV above the edge. For all measurements, data collection was done at 15 eV below and 40 eV above the edge with a step size of 0.3 eV and increments for the pre-edge was 5 eV.

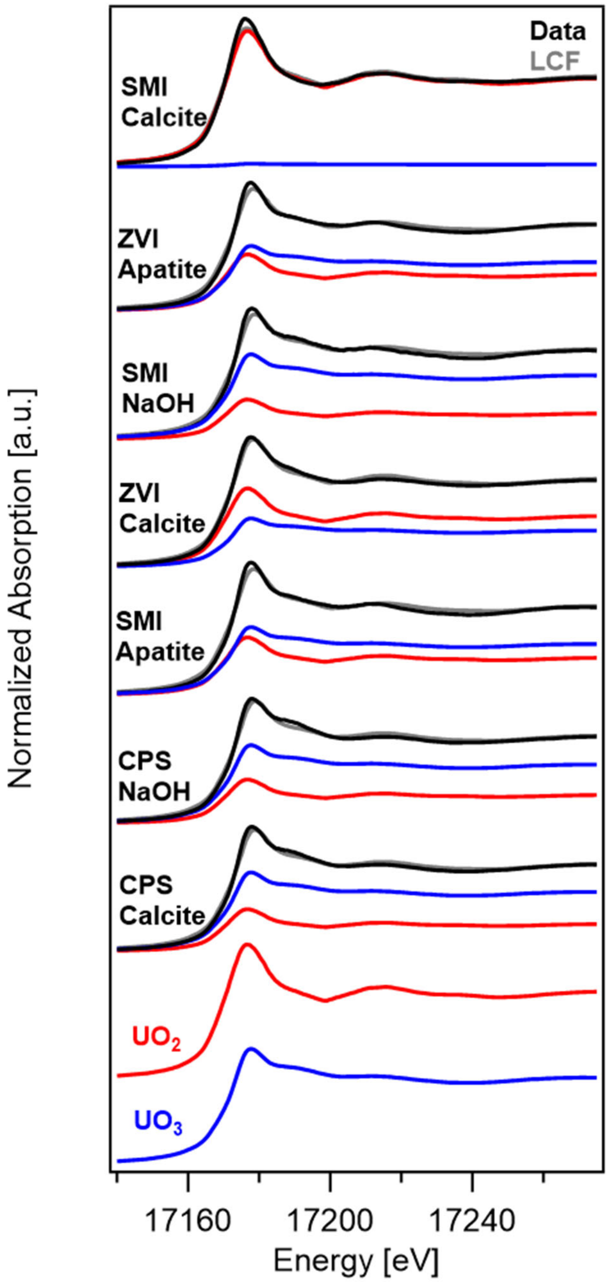

Figure A.1. LCF fit of U speciation for all analyzed samples.

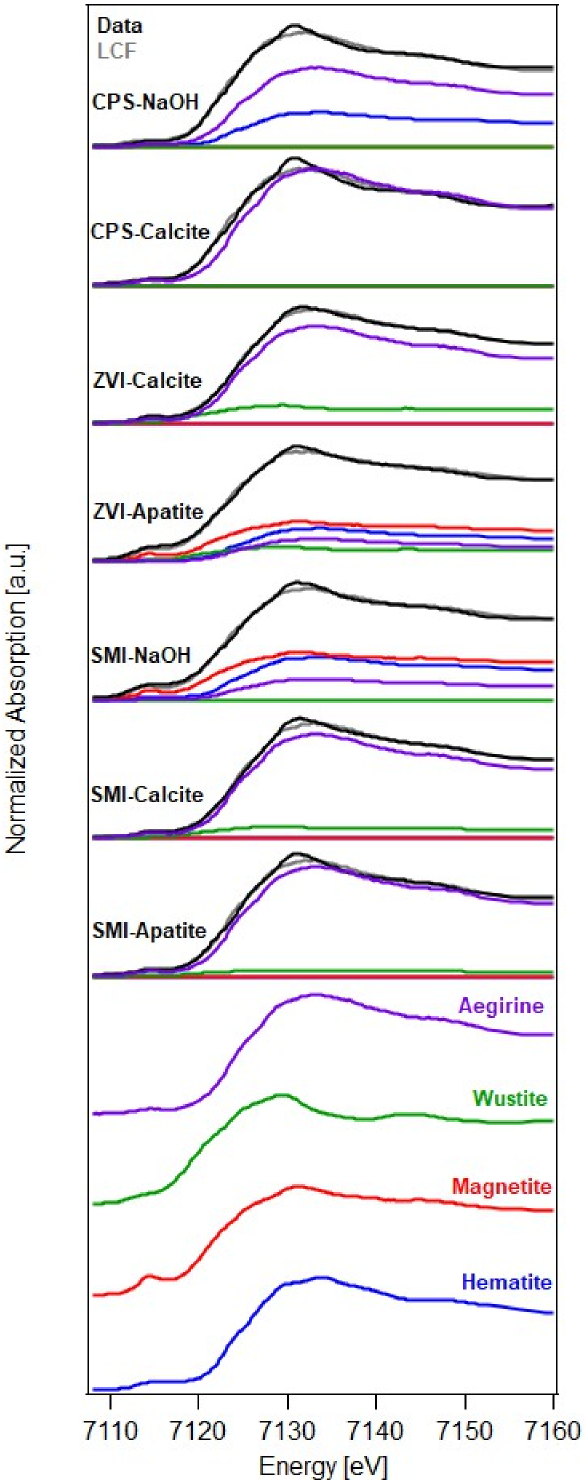

Figure A.2. Fitted Fe XANES data collected for select samples.

Pacific Northwest
National Laboratory

902 Battelle Boulevard
P.O. Box 999
Richland, WA 99354
1-888-375-PNNL (7665)

www.pnnl.gov